Science Journal of Chemistry
2023; 11(6): 197-211
http://www.sciencepublishinggroup.com/j/sjc
doi: 10.11648/j.sjc.20231106.11
ISSN: 2330-0981 (Print); ISSN: 2330-099X (Online)

Osidic Bridges of Amylose and Amylopectin Degradations by Water Molecules: Formulation of a Mechanism

N'Guessan Boka Robert, Ablé Anoh Valentin, Bamba El Hadji Sawaliho*

Laboratory of Constitution and Reaction of Matter, Unity of Formation and Research Science of Structure Matter and Technology, University Félix Houphouet-Boigny, Abidjan, Côte d'Ivoire

Email address:

nguessanbr@yahoo.fr (N'Guessan Boka Robert), ableanohvalentin@gmail.com (Ablé Anoh Valentin), bambaelhadjisawaliho@yahoo.ca (Bamba El Hadji Sawaliho)

*Corresponding author

To cite this article:

N'Guessan Boka Robert, Ablé Anoh Valentin, Bamba El Hadji Sawaliho. Osidic Bridges of Amylose and Amylopectin Degradations by Water Molecules: Formulation of a Mechanism. *Science Journal of Chemistry*. Vol. 11, No. 6, 2023, pp. 197-211. doi: 10.11648/j.sjc.20231106.11

Received: September 27, 2023; **Accepted**: October 26, 2023; **Published**: November 9, 2023

Abstract: Rapid rot of plantain causes post-harvest loss of at least 30%. It can be a source of food insecurity for consuming populations. It is linked to its polysaccharide degradation. Proposed physicochemical solutions have still not made it possible to significantly reduce this risk. Its main origin isn't considered. This compound is formed of amylose and amylopectin. Our previous works attempted to understand this process as a first step. This knowledge may facilitate the solutions to protect these polysaccharides. The mechanism of their degradation under the action of a single water molecule is simulated. Amylose with four (AM4G) or five (AM5G) building blocks is broken down into disaccharides; amylopectin with four synthons (AMP4G) into trisaccharides and with five (AMP5G) is transformed into tetra-saccharides. The destructive hydrogen bonds (HB) are located around the osidic bridge targeted by the H_2O. Higher-order oxygen seems to participate. However, this work allowed us to partially understand this mechanism. The links underlying starch splitting are not shown. The modalities of its deterioration following the simultaneous attack of two H_2O are unknown. This article aims to address these weaknesses. This research directs to establish the mechanism of starch degradation under the combined action of two H_2O. It intends to explain the connections involved in these processes. To do this, its method relies on the resources of quantum chemistry. Interactions polysaccharide-water is assessed by ONIOM method [ONIOM (B3LYP/6-311++G(d, p): AM1)]. Their energies and the electronic charge transfer are provided by the Natural Bond Orbital calculations. The geometric, energetic, spectroscopic parameters of the molecules and the electron density are generated with Gaussian09. The preferred HB sites for AM4G or AMP4G are respectively O37 (O_{2sp3}) and O63 (O'_{3sp3}). Oxygen O37 (O_{2sp3}) is an HB anchor for AM5G. O14 (O'_{1sp3}) and O86 (O'_{4sp3}) are for those of AMP5G. In addition, amylose is degraded before the latter. The division of the complexes into several bonds results from the interactions of the H_2O on the different saccharide bridges of the synthons. Thus, the O14-C25, O37-C46 and O58-C67 are involved in the cleavage of AM4G. The O13-C21, O55-C65 and O63-C43 are in that of AMP4G. The O14-C25, O37-C46 and C50-O58 and O79-C107 are associated with that of AM5G. O14-C25, O35-C44, O78-C88 and C30-O86 are those connected to AMP5G.

Keywords: Starch, ONIOM, NBO Analysis, Hydrogen Bonds, Amylose and Amylopectin

1. Introduction

Rapid plantain rot is a global concern; it causes a post-harvest loss of at least 30% [1]. It is linked to the degradation of its polysaccharides [2]. In addition, populations who consume this fruit could be led to food insecurity [3]. According to [4], physicochemical solutions have been used to extend the green life of bananas. They remain ineffective. The deterioration of its starch is not considered. This compound is made up of amylose and amylopectin. Previous work was carried out to discover the mechanism of their degradation under the action of a single water molecule [4, 5]. For [6], amylose with four (AM4G) or five (AM5G) synthons was disintegrated into disaccharides. Four-unit amylopectin (AMP4G) was decomposed to

trisaccharides. That of five synthons (AMP5G) was transformed into tetra-saccharides. Furthermore, the destructive hydrogen bonds were located around the target saccharide bridge. However, this work allows us to partially understand this mechanism of polysaccharide division.

The links underlying starch splitting are not shown. The modalities of its degradation following the simultaneous attack of two water molecules are unknown. This research aims to fill these gaps through this question:

What are the atoms and bonds around which the split into amylose and amylopectin takes place under the action of one or two water molecules?

The research assumes that the division of polysaccharides under the action of two water molecules takes place around their saccharide bridges close to them. The resources of quantum chemistry were mobilized to answer this question and test this hypothesis.

Interactions in polysaccharide-water complexes are evaluated by the two-layer method of Own N-layered Integrated molecular Orbital and molecular Mechanics (ONIOM) [ONIOM (B3LYP/6-311++G (d, p): AM1)]. Their energies and electronic charge transfer (C.T) are provided by Natural Bond Orbital (NBO) calculations. The geometric, energetic and spectroscopic parameters of the molecules and the electron density (E.D) are generated using Gaussian09. This methodological approach made it possible to carry out the next computations.

The degradation of amylum or amylopectin under the action of two H_2O is studied. Its order according to the sizes of these compounds is examined. The connections involved in these processes are analyzed. Their parameters are clarified. The following results are established. The major HB sites of polysaccharides were determined for amylose and amylopectin with AM4G or AMP4G (four α-D-glucose synthons) respectively. Those of AM5G (five-synthon amylose) or AMP5G (five-synthon amylopectin) are revealed. Their cleavage modalities under the effect of H_2O are described. Furthermore, the links involved in this divide are explained. This article is organized to five parts.

After this introduction, the calculation strategies are summarized. Then, the study of the parameters is detailed. The results are presented and discussed. The paper ends with a conclusion.

2. Calculation Strategies

The calculation method is presented in this section. The means utilized to access the geometric, energetic, and spectroscopic parameters are shown. The NBO analysis technic and the exploitation of the interaction potential are explained. Before, the polysaccharides are described.

2.1. Study Compounds

The 3D molecular structure of AM4G (four α-D-glucose synthons of amylose), AM5G (five α-D-glucose synthons of amylose), AMP4G (four α-D-glucose synthons of amylopectin) and AMP5G (five α-D-glucose synthons of amylopectin) were examined [6]. All oxygen atoms were sp^3 hybridized. The osidic bridges were numbered from 1 to 3 for the tetrasaccharides and from 1 to 4 for the pentasaccharides.

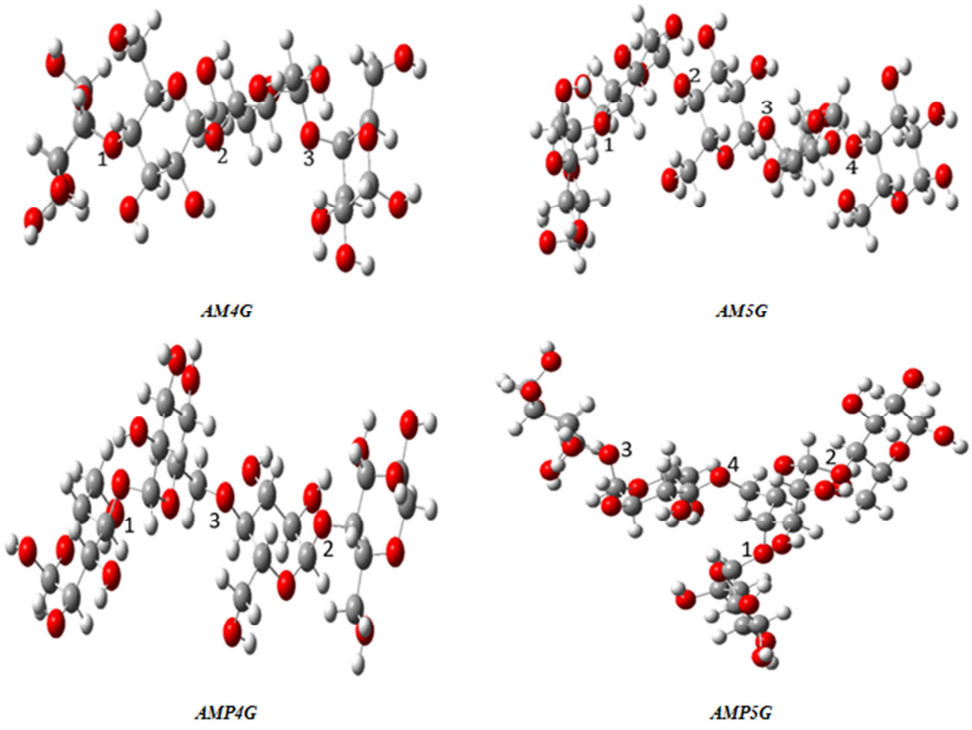

Figure 1. *3D Image of the AM4G, AM5G, AMP4G and AMP5G.*

2.2. Calculation Methods

An ONIOM technique was employed to optimize molecular structures. It is based on the work of Chung and al (2012) cited by [7]. The amylose or the amylopectin HB site of the detection was used in our previous research [6]. Chemical entities were studied by this approach. A complex is divided into two portions. These can be understood at different levels of calculation. The groupings adopted for the estimations are presented in Figure 2. The water molecules are moved to every oxygen in the osidic bridges. The first part (internal) is circled. It is composed of atoms connected to the bridge. The HB will be precisely described inside this division. A high degree (B3LYP/6-311++G (d, p)) of the computations are performed; diffuse and polarization functions are required to consider isolated oxygen pairs and their interactions with hydrogen in H_2O. For the second (outer) portion, the remaining section of the molecule is determined by a less rigorous semi-empirical AM1 approach.

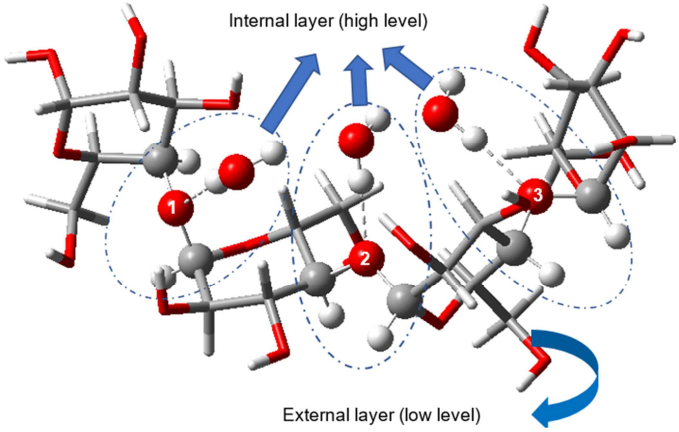

Figure 2. *Calculation Diagram According to the ONIOM Method.*

The energy of the system at a high level (the circled part in Figure 2) is evaluated: E (DFT, model). That of the complex at AM1 degree (the entire complex in Figure 2) is determined: E (AM1, complex). At the previous degree, the energy is calculated: E (AM1, model). Finally, that of the complex (polysaccharide) is computed: E (DFT, polysaccharides). It was calculated with the equation 1.

$$\text{E (DFT, polysaccharide)} = \text{E (AM1, complex)} + \text{E (DFT, model)} - \text{E (AM1, model)} \quad (1)$$

The achieved structures were justified by the NBO calculations. The electronic transitions were obtained. They are characterized by their stabilizing energies E^2. These resulted from the second-order perturbation theory. They are associated with the electronic delocalization between the HB [8]. The stabilization energy is given by the formula below (equation 2)

$$E^2 = q_i \frac{(F_{i,j})^2}{\varepsilon_i - \varepsilon_j} \quad (2)$$

The clear information on the stabilization process of the complexes was provided by E^2. The strength of the HB was reflected. The higher E^2 is, the stronger is the associated HB interaction. The atoms of the complex involved in this interaction became the preferred situs for establishing an HB within the synthon. They constituted the starting points for the breaking of the polysaccharides. All calculations were implemented by the Gaussian 09 software [9]. Their geometries, their thermodynamic and spectroscopic parameters were generated. They are presented in the next section.

3. Study Parameters

The polysaccharide order of degradation is discussed with energy quantities. Three categories of parameters were involved. The validation of the HB site's geometrical characteristics is based on spectroscopic data. These are described in the following section.

3.1. Geometric Parameters of the Hydrogen Bond

The complex is built by linking hydrogen from water to each oxygen of the osidic bridge. The HB formed is characterized by three geometric quantities (Figure 3). Before polysaccharide optimization, the linearity angle α is fixed at 180°. The hybridization state of the oxygen is sp^3; β is equalled to 109.5° (Figure 4). The distance d between the last atom to hydrogen is 2 Å. It is corresponded to their minimum approach length [10].

According to [11], HB is probably occurred when the distance d became less than the Van der Waals radii sum of the oxygen (1.52 Å) and hydrogen (1.1 Å) [12-13]. This criterion is summarized as $d \leq 2.62$ Å. The HB is mutated strong as d decreases; its smallest value is the preferred osidic site. The space between the O…H and the Y-A bonds is represented by the angle α; A is the acceptor atom. It is lied between the Y-A and the HO links on the HB. The more α is deviated from its ideal worth, the more this last is destabilized. However, the more this angle is opened, the more the establishment of HB is favoured. Moreover, HB is also

described by energetic parameters.

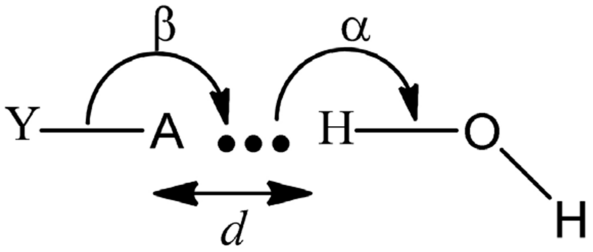

Figure 3. *HB Parameters α, β and d of the HB [14].*

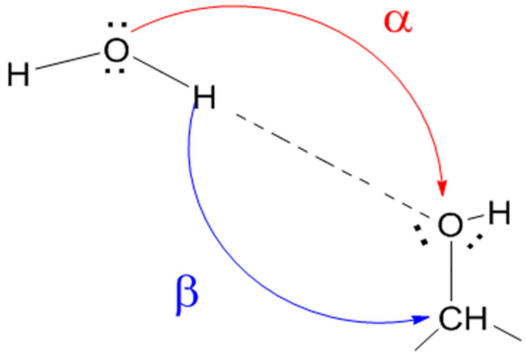

A=180°; oxygen sp^3; β=109.5°

Figure 4. *Linearity and Direction Angles of the HB.*

3.2. Energy and Thermodynamic Parameters of the Hydrogen Bond

The HB between an H-X donor and a Y-A proton acceptor take place as Equation 3 is shown. Its product is the Y-A…H-X complex.

$$Y - A + H - X \rightarrow Y - A \cdots H - X \quad (3)$$

The change in energy at 0 K is obtained from equation 4:

$$\Delta E^0_{elec} = E^0_{elec}\,(Y - A \cdots H - X) - [E^0_{elec}(Y - A) + E^0_{elec}(H - X)] \quad (4)$$

The internal energy at 298.15 K is the sum of the electronic, rotational, translational, and vibrational ones. Its variation is described by equation 5:

$$\Delta E^0_{298} = \Delta E^0_{electronic} + \Delta E^0_{rotational} + \Delta E^0_{translational} + \Delta E^0_{vibrational} \quad (5)$$

All the contributions (including the nuclear repulsion energies) are accessed by optimizing the geometry of the reactants and the products. In the ideal gas approximation, the expressions for the rotational and translational energies of the molecules are presented by equation 6:

$$\Delta E^0_{translational} = \Delta E^0_{rotational} = -\frac{3}{2}RT \quad (6)$$

The ZPVE (Zero Point Vibrational Energy) is included in the $\Delta E^0_{vibrational}$. The 3N-6 normal modes (3N-5 for linear molecules) contributed to it. Each one has a frequency ν_i, at 0 K. Its $E^0_{vib.thermal}$ at this temperature is defined by Equation 7:

$$E^0_{vib.thermal} = R\sum_{i=1}^{3N-6} \frac{h\nu_i/k}{e^{h\nu_{i/298K}} - 1} \quad (7)$$

Consequently, the change in internal energy of the reaction at 298.15 K is given by equation 8:

$$\Delta E^0_{298} = \Delta E^0_{elec} + \Delta ZPVE + \Delta E^0_{vib.thermal} - 3RT \quad (8)$$

The enthalpy and the free enthalpy changes for the reaction of complexation at 298.15 K are respectively specified by equations 9 and 10:

$$\Delta H^0_{298K} = \Delta E^0_{298K} - RT \quad (9)$$

$$\Delta G^0_{298K} = \Delta H^0_{298K} - T\Delta S^0_{298K} \quad (10)$$

$$\Delta S^0_{298K} = \Delta S^0_{trans} + \Delta S^0_{rot} + \Delta S^0_{vib} \quad (11)$$

The entropy variation is provided by Equation 11 under these conditions. In addition, the sites of polysaccharide HB interactions are identified by spectroscopic parameters.

3.3. Spectroscopic Parameters of the Hydrogen Bond Abbreviations

Spectroscopic descriptors are often used as a scale for HB. The strength of a H-X is depended on that of this link. Its stretch frequency is accessible. When the donor is a water molecule, the displacement $\Delta\vartheta_{O-H}$ became the scale. For the sp^3 osidic oxygen, it is defined by equation 12:

$$\Delta\vartheta_{O-H} = \vartheta(O_{sp^3} - H, free) - \vartheta(O_{sp^3} - H, complex) \quad (12)$$

At the ONIOM level (B3LYP/6-311++G(d, p): AM1), the vibrator frequency $\vartheta(O_{sp^3} - H, free)$ is equalled to 3923.84 cm^{-1}. If the value $\Delta\vartheta_{O-H}$ is positive, that of $\vartheta(O_{sp^3} - H, complex)$ is converted less than $\vartheta(O_{sp^3} - H, free)$; the frequency $\vartheta(O_{sp^3} - H, free)$ of the water decreased. The oxygen of the osidic bridge was approached by its hydrogen. Simply, as $\Delta\vartheta_{O-H}$ is increased, it is probably transformed to a site likely to favour an HB. The results for four- and five-synthon polysaccharides are discussed.

4. Results and Discussion

The pentasaccharide geometric, energetic, and spectroscopic parameters are described below. Those dedicated to the implementation of NBO calculations are shown. The effects of H_2O on the atoms associated with the osidic bridges within complexes are detailed.

4.1. Study of Polysaccharides with Four Synthons

The complexes formed from AM4G and AMP4G with one and two water molecules on each of these three bridges was emphasized on. Their geometric parameters were spotlighted.

4.1.1. Geometric Parameters Primarily

The optimized geometries at ONIOM level (B3LYP/6-311++G (d, p): AM1) for AM4G-3H_2O, AM4G-(3H_2O)$_2$, AMP4G–3H_2O and AMP4G—(3H_2O)$_2$ are shown in Figure 5. Their parameters are listed in Table 1.

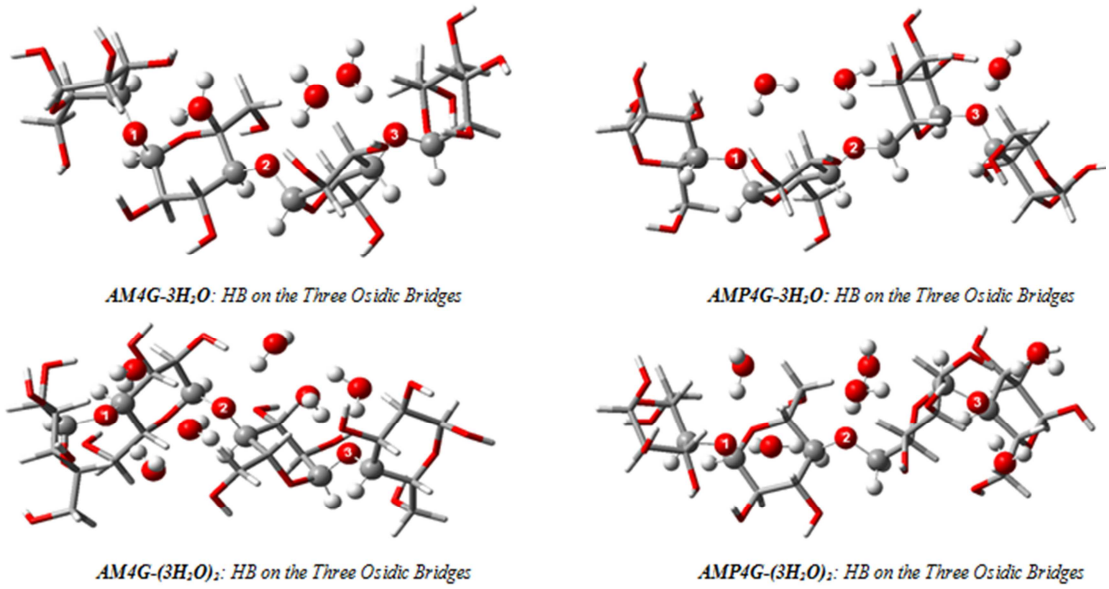

Figure 5. *Optimized geometries of the Complexes at ONIOM Level (B3LYP/6-311++G(d, p): AM1).*

All d-lengths remained below 2.62 Å; an HB was both established by the three osidic oxygen and the attraction of a water molecule hydrogen. The shortest (1,818 Å) was created with the O37 atom of the AM4G-3H_2O complex. It was also the strongest. The α-linearity of this interaction was the closest to 180°. It was accompanied by the direction angle β much nearer to 109.5 °. Its other two HB were too stable. That of the O14 oxygen was the second solidest. Their parameters α and β were weakly deviated from the ideal values. Its d (1,931 Å) was shorter than that of O58 atom (1,978 Å). These HB can be ranked in descending order of strength through the osidic bridges O63> O14> O58. All the d-lengths in the AMP4G-3H_2O complex were less than 2 Å. The HB established with the O63 atom was the smallest. It has been preceded by the O13 oxygen and finally by the O58 one. The other two geometric parameters were perturbed by steric hindrances.

Table 1. *Geometric Parameters of AM4G-3H_2O and AMP4G—3H_2O Complexes at ONIOM Level (B3LYP/6–311++G(d, p): AM1).*

AM4G-3H_2O	α (°)	β (°)	d (Å)	AMP4G-3H_2O	α (°)	β (°)	d (Å)
O14 (O_{1sp3})	172.152	126.390	1.931	O13 (O'_{1sp3})	165.518	117.830	1.839
O37 (O_{2sp3})	175.706	112.849	1.818	O55 (O'_{2sp3})	169.198	110.309	1.921
O58 (O_{3sp3})	173.415	118.231	1.978	O63 (O'_{3sp3})	164.047	125.234	1.809

The α-linearity and β-direction angles of O58 were respectively close to 180° and 109.5 °. However, this HB was the least strong because of its long-distance (1,921 Å). So, all the HB were stable. The solidest was occurred with O37 oxygen (O_2sp^3) (d = 1,818 Å) in AM4G—3H_2O and with O63 atom (O'_3sp^3) (d = 1,809 Å) in AMP4G—3H_2O. These two sites had the lowest d values. They were contributed to the robustness of HB. Finally, the O37 (O_2sp^3) and O63 (O'_3sp^3) atom were respectively the main HB anchor points for AM4G-3H_2O and AMP4G-3H_2O. These results were consistent with those obtained by [6]. The energetic parameters of the different complexes are discussed. They are summarized in Table 2.

Table 2. *Energy Parameters (in kcal/mol) and Entropy (cal/mol. K^{-1}) of the AM4G—3H_2O and AMP4G—3H_2O Complexes.*

Complexes	$\Delta_rH°_{298}$	$\Delta_rS°_{298}$	$\Delta_rG°_{298}$
AM4G-3H_2O	-26.755	-111.178	6.393
AMP4G-3H_2O	-21.464	-96.148	7.203
Variations des grandeurs	5.291	15.030	0.810

4.1.2. Energy Parameters

The AM4G—3H_2O and AMP4G—3H_2O energy parameters are described. The values of the enthalpies $\Delta_rH°_{298}$ were negative; the HB formation processes were exothermic. The O-H bonds frequency differences between the AM4G and AMP4G structures and those of their complexes corresponded to the variations. They were the basis of the following results.

The AM4G-3H_2O was more stable than AMP4G-3H_2O; the free enthalpies of reaction were deviated by 5,291 kcal/mol. Its change was small (0.810 kcal/mol). The degradation process of the AM4G was made easy compared to that of the AMP4G. For the same molecular weight, the alteration of amylopectin was slower than that of amylose. In addition, the spectroscopic parameters are analyzed.

4.1.3. Spectroscopic Parameters

The O-H stretching difference vibrational frequencies in the AM4G and AMP4G structures and in those of their complexes were designed by the Δϑ(O-H) variations. The last are grouped in Table 3. Their diverse osidic bridges are indicated.

Table 3. *Vibration Frequencies* $\Delta\vartheta_{O-H}$ *(cm^{-1}) of AM4G—3H$_2$O and AMP4G—3H$_2$O Complexes at ONIOM Level (B3LYP/6-311++G(d,p): AM1).*

AM4G	Δϑ (O–H) (cm^{-1})	AMP4G	Δϑ (O–H) (cm^{-1})
O14 (O$_1$sp^3)	294.85	O13 (O'$_1$sp^3)	295.53
O37 (O$_2$sp^3)	302.39	O55 (O'$_2$sp^3)	246.4
O58 (O$_3$sp^3)	259.51	O63 (O'$_3$sp^3)	379.42

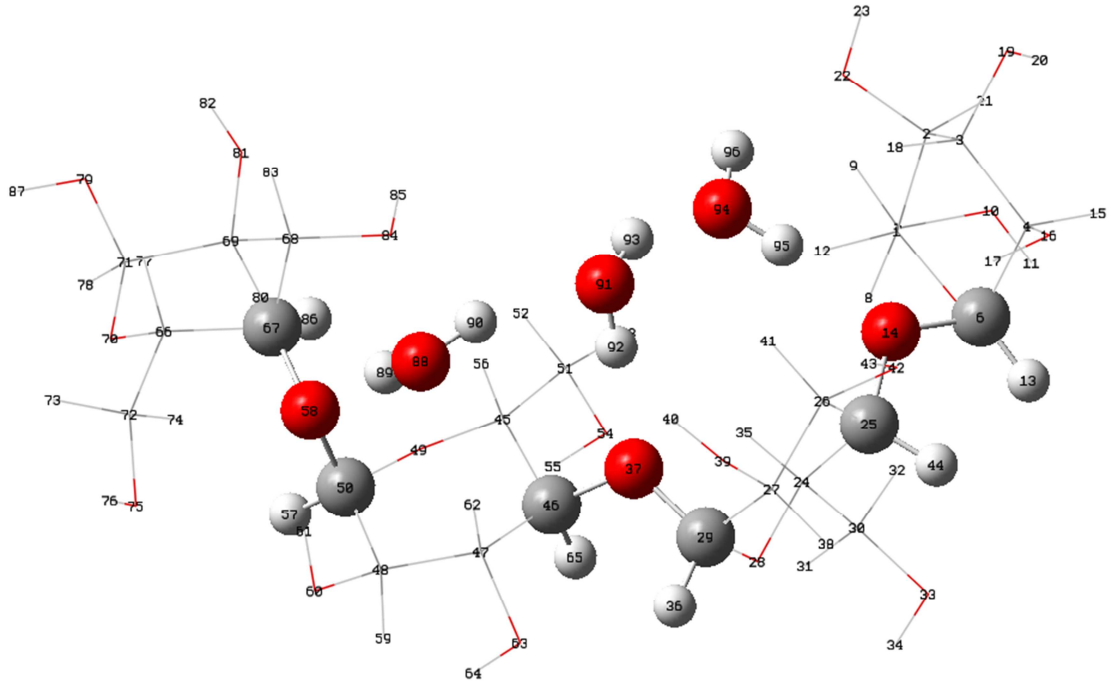

AM4G-3H$_2$O

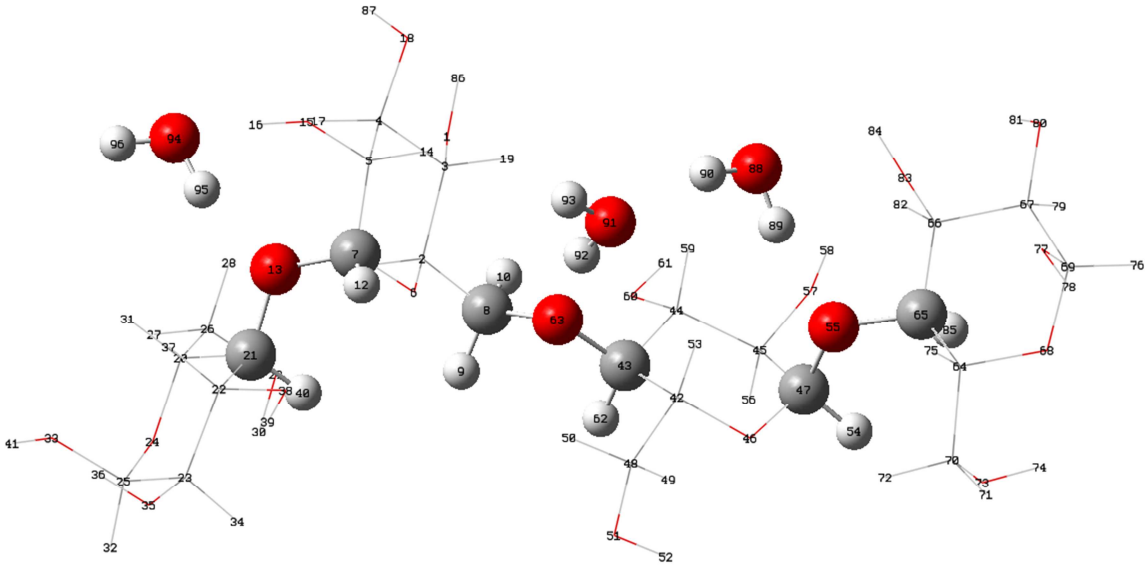

AMP4G-3H$_2$O

Figure 6. *Gauss Views 06 Software Numbering Adopted for NBO Analysis of AM4G—3H$_2$O and AMP4G—3H$_2$O Complexes.*

The Δϑ(O-H) variations were positive. Those of the O37 (O$_2$sp^3) and O63 (O'_{3sp3}) oxygen of AM4G and AMP4G corresponded to the highest values. Their frequencies were respectively 302.39 cm^{-1} and 379.42 cm^{-1}. The O37 (O$_2$sp^3) and O63 (O'_{3sp3}) atoms became the preferred sites for establishing HB with AM4G and AMP4G. A previous finding of the team was corroborated [6]. Furthermore, the NBO method was applied.

4.1.4. NBO Analysis Applied to Amylose or Amylopectin Complexes of Four Synthons

The inter- and intramolecular interactions of the

AM4G—$3H_2O$ and AMP4G-$3H_2O$ complexes were examined by the NBO analysis. Their atomic numbers were shown in Figure 6. The results of the calculations are recorded in Tables 4 and 6. They were restricted to those linked to their osidic bridges.

(i). NBO Analysis of the AM4G—$3H_2O$ and AMP4G—$3H_2O$ Complexes Intermolecular Interactions

The most important intermolecular C.T for the AM4G-$3H_2O$ was observed with the osidic bridge O37. The interaction $LP_1\ (O_{37}) \rightarrow \sigma^*(O_{91} - H_{92})$ was associated with the latter. The stabilization energy E^2= 9.05 kcal/mol was accompanied by a C.T of 14.50 a.u. The HB on the O37 with the water being the strongest. Its free pairs were available for this formation; the E.D was equalled to 1.94590e around it. The preferred site for establishing HB with AM4G was the O37 atom. For AMP4G—$3H_2O$, the most important intermolecular C.T came from the O63 osidic bridge. The interaction $LP_1\ (O_{63}) \rightarrow \sigma^*(O_{91} - H_{92})$ was associated with it. Its stabilization energy E^2 = 8.90 kcal/mol was related to an electronic C.T of 14.17 a.u. The HB established on this oxygen with the water was strong. Its free pair in this direction was available; its E.D around the O63 was worth to 1.94673e. This mentioned atom became the main anchor point for HB with AMP4G. The first cleavage of AM4G and AMP4G were respectively begun at their O37 and O63 heteroatoms. This result was consistent with the conclusions drawn in the previous sections. AM4G and AMP4G were preliminarily slit into disaccharides. After, the weathering process was continued until monosaccharides was obtained. The geometric, energetic, and spectroscopic parameters were examined. Then, NBO analysis followed. The preferred HB receptors for the AM4G, and AMP4G polysaccharides were respectively the O37 (O_2sp^3) and O63 (O'_{3sp3}) oxygen. The results related to the different complexes are summarized in Table 5.

Table 4. *Second-order perturbation energies E^2 (Kcal/mol), C.T and E. D for intermolecular transitions in the AM4G—$3H_2O$ and AMP4G—$3H_2O$ Complexes.*

	Intermolecular interactions between AM4G—H_2O and AMP4G—H_2O									
	NBO DONOR (i)			**NBO ACCEPTOR (j)**						
Complexes	**Donor**	**Type**	**E.D (electron)**	**Acceptor**	**Type**	**E. D (electron)**	**E^2 (kcal/mol)**	**E. (j)—E. (i) (a. u)**	**F (i, j) (a. u)**	**C.T 10^3 (a. u)****
AM4G –$3H_2O$	FP* (1) O14	Π	1.95059	O94-H95	σ*	1.99416	5.79	0.99	0.068	9.44
	FP(2) O14	Σ	1.91510	O94-H95	σ*	1.99416	0.79	0.76	0.022	1.68
	FP(1) O37	Π	1.94590	O91-H92	σ*	1.99388	9.05	1.01	0.086	14.50
	FP(2) O37	Σ	1.91723	O91-H92	σ*	1.99388	1.79	0.77	0.034	3.90
	FP(1) O58	Π	1.95733	O88-H89	σ*	1.99542	3.95	1.04	0.057	6.01
	FP(2) O58	Σ	1.91277	O88-H89	σ*	1.99542	2.34	0.78	0.039	5.00
AMP4G-$3H_2O$	FP(1) O13	Π	1.94939	O94-H95	σ*	1.99510	6.53	0.97	0.071	10.72
	FP(2) O13	Σ	1.93271	O94-H95	σ*	1.99510	4.93	0.79	0.056	10.05
	FP(1) O55	Π	1.95218	O88-H89	σ*	1.99481	5.32	1.04	0.067	8.30
	FP(2) O55	Σ	1.92107	O88-H89	σ*	1.99481	1.37	0.78	0.030	2.96
	FP(1) O63	Π	1.94673	O91-H92	σ*	1.99501	8.90	1.01	0.085	14.17
	FP(2) O63	Σ	1.92300	O91-H92	σ*	1.99501	0.33	0.75	0.014	0.70

Table 5. *Key Research Findings Associated with AMP4G and AMP4G.*

Associated criteria	**Most likely site of the HB for AM4G**	**Most likely site of the HB for AMP4G**
Geometry: distance	O37 (O_2sp^3)	O63 (O'_3sp^3)
Enthalpy	AM4G was degraded more easily than AMP4G	
Free enthalpy	HB formation is not spontaneous	
Spectroscopy	O37 (O_2sp^3)	O63 (O'_3sp^3)
NBO analysis: intermolecular	O37 (O_2sp^3)	O63 (O'_3sp^3)
Result	O37 (O_2sp^3)	O63 (O'_3sp^3)

(ii). NBO Analysis of the AM4G—$3H_2O$ and AMP4G—$3H_2O$ Intermolecular Interactions

The E.D around the bonds of the osidic bridges are displayed in Table 6. The intramolecular interactions were identified. For AM4G, according to the minimum D.E rule, three breaks were occurred. The first happened with O14; it concerned the O14-C25. Its E.D. = 1.98422e was lower than that linked to C6-O14; the weak availability of electrons was reflected. The two breakpoints were in the order of precedence O37 from O37-C46 followed by O58 from O58-C67. The E. D. associated with their intramolecular interactions were 1.98571e and 1.98616e respectively. A similar reasoning was led to the preferred cut-offs for AMP4G. The oxygen O13 (O13-C21), O55 (O55-C65) and O63 (O63-C43) represented them. In this order, their E.D. was around 1.98536e, 1.98444e and 1.98476e. The main anchoring sites of HB within the synthons through intermolecular dynamics were identified by the NBO analysis. In addition, the linkages that contributed to the degradation of polysaccharides were highlighted. Moreover, the effects of water molecules on geometry were investigated. Specifically, the concomitant actions of two on each osidic bridge are detailed in the section.

Table 6. *E.D (in electron) Associated with the Osidic Bridges' Intramolecular Bonds of AM4G or AMP4G.*

Molecule	Sites	Link	Type	E.D. (electron)
AM4G	O14	C6-O14	Σ	1.98847
		O14-C25	Σ	1.98422
	O37	C29-O37	Σ	1.98823
		O37-C46	Σ	1.98571
	O58	C50-O58	Σ	1.98768
		O58-C67	Σ	1.98616
AMP4G	O13	C7-O13	Σ	1.98782
		O13-C21	Σ	1.98536
	O55	C47-O55	Σ	1.98791
		O55-C65	Σ	1.98444
	O63	C8-O63	Σ	1.98743
		O63-C43	Σ	1.98476

4.1.5. Geometry of Complexes AM4G— $(3H_2O)_2$ and AMP4G — $(3H_2O)_2$

Each osidic bridge concomitantly interacted with two H_2O. The effects of this reaction between polysaccharides and the last are focused on this section. These complexes were formulated as AM4G-$(3H_2O)_2$ and AMP4G-$(3H_2O)_2$.

(i). Complexes Associated with Amylose

The bond lengths and valence angles associated with osidic oxygen are summarized in Table 7. The contribution of water molecules to the splitting at its bridge is discussed. The changes of the second variable were tiny compared to those of the free AM4G. Their openings remained identical to that of O37 when interacting with one or two H_2O. For the O58, these angles had approximately the same values. For those centred on the O14, the spacing was 0.94° with one H_2O and the closing was 2.66° when approaching two. Those of O37 were related to the strength of the HB. These geometrical situations had predisposed the non-bonding doublets of this atom to C.T as shown by the NBO analysis.

Table 7. *Bond Lengths d (Å) and Valence Angles θ (°) Related to the Osidic Bridges of AM4G, AM4G—H_2O and AM4G—$2H_2O$.*

Distances	Angles	AM4G	AM4G-H_2O	AM4G-$2H_2O$	Δd_1	$\Delta\theta_1$	Δd_2	$\Delta\theta_2$
d (C6-O14)		1.42	1.43	1.45	0.01		0.03	
d(O14-C25)		1.42	1.45	1.45	0.02		0.03	
	θ(C-O-C)	118.99	119.93	116.33		0.94		-2.66
d(C29-O37)		1.43	1.43	1.42	0.00		0.00	
d(O37-C46)		1.43	1.44	1.44	0.01		0.01	
	θ(C-O-C)	115.93	117.58	117.42		1.64		1.49
d(C50-O58)		1.41	1.43	1.44	0.02		0.02	
d(O58-C67)		1.43	1.44	1.44	0.01		0.01	
	θ(C-O-C)	119.38	116.63	116.73		-2.75		-2.64

Regarding the O14 atom, the greatest stretching was at O14-C25. This bond was acquired Δd_1 = 0.02 Å. Its length was increased as two molecules of H_2O was approached. It was improved by Δd_2 = 0.03 Å. The cleavage of the O14 saccharide bridge was begun with O14-C25. For the O37, the O37-C46 link in the AM4G-H_2O complex was prolonged of Δd_1 = 0.01 Å. It was grown by Δd_2 = 0.01 Å when two waters were interacted simultaneously on this bridge. AM4G broke at the O37-C46. For the O58, the greatest rise in length was occurred. It was equivalent to Δd_1 = 0.02 Å. The variation Δd2 = 0.02 Å was reached in the concomitant presence of H_2O. The rupture of the O58 was taken place around the C50-O58. The first two results were corroborated by those of the NBO. They remained the basis for the AM4G split. Moreover, the valence angles on the different osidic bridges changed slightly when the last was approached by a water molecule.

These angles were $\Delta\theta_1$ = 0.94°, $\Delta\theta_1$ = 1.64° and $\Delta\theta_1$ = -2.75°. They were related to the oxygen O14, 037 or O58. This trend was maintained by the addition of another H_2O. The angular displacements became $\Delta\theta_2$=-2.66°, $\Delta\theta_2$ = 1.49° and $\Delta\theta_2$ = -2.65°. This geometric parameter was remained irrelevant for determining the bond breakage points of amylose; the data associated with AM4G was stable. The effects of water molecules on amylopectin consisting of four synthons (AMP4G) are also examined.

(ii). Complexes Associated with Amylopectin

The bond lengths between the carbon and the osidic oxygen and the valence angles are grouped in Table 8. The simultaneous dynamic between H_2O and each second atom had increased them. In the case of the O13, the O13-C21 binding was impacted; the variation was attained Δd_1 = 0.01 Å. It was intensified when associating with two water molecules. It was acquired Δd_2 = 0.01 Å. The alteration at sites O13 was started from the O13-C21. For O55, the concerned link was O55-C65; its displacement in AMP4G-H_2O had reached Δd_1 = 0.01 Å. It was increased by Δd_2 = 0.02 Å when two H_2O was connected on O55; The O55-C65 became the breaking point of this osidic bridge. For O63, the greatest value of Δd1 occurred near O63-C43 (0.01 Å) in AMP4G-H_2O. The interaction of two water molecules at this location was lengthened C8-O63 by Δd2 = 0.01 Å. The rupture of the O63 bridge happened around the C8-O63 bond. Moreover, the predictions deduced from the NBO analysis were confirmed by these results. However, this last method was not advocated by those associated with the C8-O63 binding.

Table 8. *Bond Lengths d (Å) and Valence Angles θ (°) Related to the Osidic Bridges of the AMP4G, AMP4G—H_2O and AMP4G—$2H_2O$.*

Distances	Angles	AMP4G	AMP4G-H_2O	AMP4G-$2H_2O$	Δd_1	$\Delta\theta_1$	Δd_2	$\Delta\theta_2$
d(C7-O13)		1.43	1.44	1.45	0.01		0.02	
d(O13-C21)		1.43	1.44	1.44	0.01		0.01	

Distances	Angles	AMP4G	AMP4G-H_2O	AMP4G-2H_2O	Δd_1	$\Delta\theta_1$	Δd_2	$\Delta\theta_2$
	θ(C-O-C)	116.00	116.31	116.12		0.31		0.11
d(C47-O55)		1.43	1.44	1.45	0.01		0.02	
d(O55-C65)		1.43	1.44	1.45	0.01		0.02	
	θ(C-O-C)	113.94	117.41	116.75		3.46		2.80
d(C8-O63)		1.43	1.44	1.44	0.01		0.01	
d(O63-C43)		1.44	1.44	1.44	0.01		0.01	
	θ(C-O-C)	117.66	114.71	113.86		-2.95		-3.79

The results of the NBO analysis relating to intramolecular interactions are summarized in Table 9. Those associated with the effects of water on the osidic bridge atoms of AM4G or AMP4G are presented. After studying the four building blocks of amylose and amylopectin, the research elucidated the order of their cleavage. Figure 7 illustrated them. In addition, this work also dealt with those with five synthons.

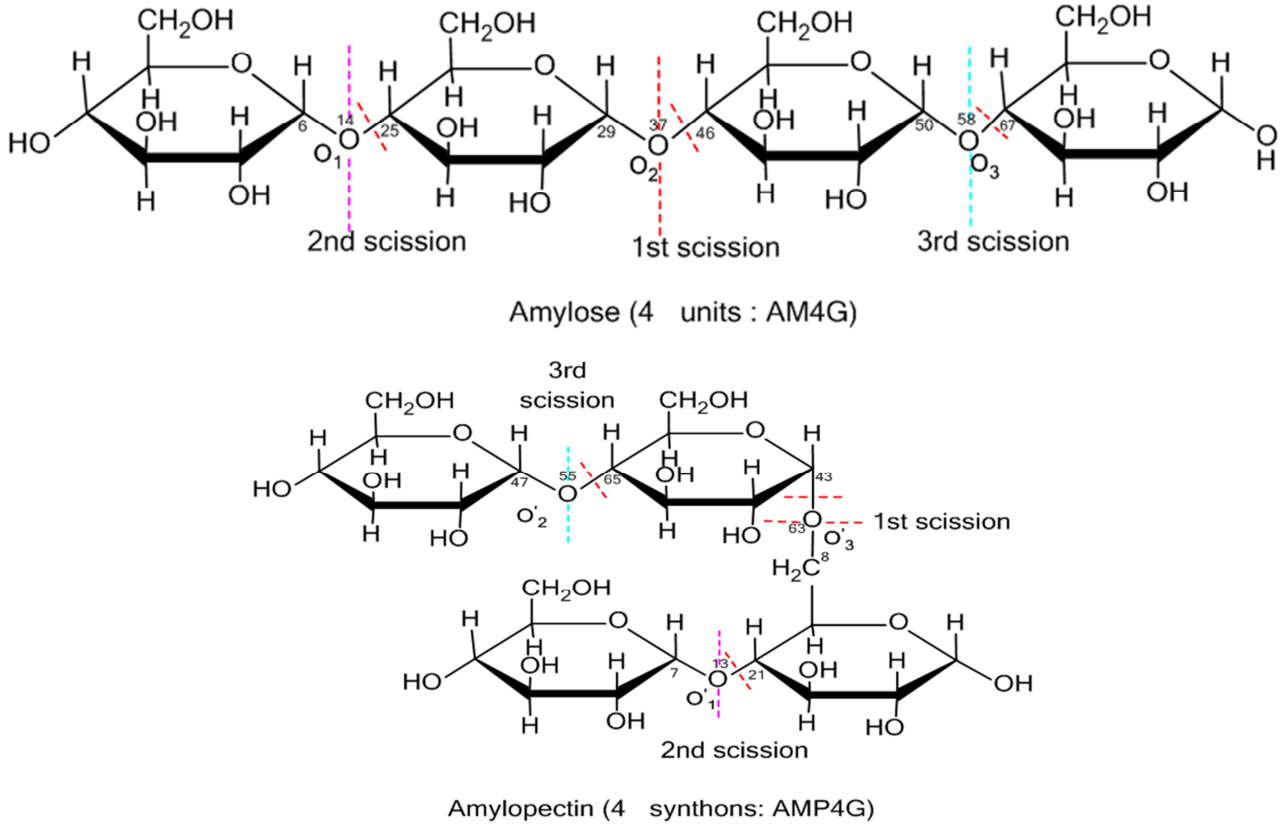

Figure 7. *Scission Order of Amylose and Amylopectin with Four Synthons.*

Table 9. *Key Research Findings Associated with the AMP4G-H_2O and AMP4G-2H_2O Complexes.*

Associated criteria	Links involved in the AM4G split	Links involved in the AMP4G split
NBO analysis: intramolecular	O14-C25, O37-C46 and O58-C67	O13-C21, O55-C65 and O63-C43
Effects of H_2O	O14-C25, O37-C46 and C50-O58	O13-C21, O55-C65 and C8-O63
Results	O14-C25, O37-C46 and O58-C67	O13-C21, O55-C65 and O63-C43

4.2. Polysaccharides Composed of Five Synthons

The study was focused on complexes of AM5G and AMP5G with one and two water molecules on each osidic bridge. First, their geometrical parameters were examined.

4.2.1. Geometry Parameters

The optimized geometries at ONIOM level (B3LYP/6-311++G (d, p): AM1) for AM5G—4H_2O, AM5G — (4H_2O)$_2$, AMP5G—(4H_2O)$_2$ and AMP5G — (4H_2O)$_2$ are shown in Figure 8. Their calculated geometrical parameters are displayed in Table 10. The d values were less than 2.62 Å. The four oxygen of the saccharide bridges was established HB by an attraction of the water hydrogen. The linearity angles α and direction β was closed to 180° and 109.5°. All the HB were stable. However, the strongest HB was achieved with O37 (O_2sp^3) (d = 1,825 Å) in AM5G—4H_2O and O86 (O'_{4sp3}) (d = 1,874 Å) in AMP5G—4H_2O. These two sites had the lowest d values. They participated in the solid HB. Finally, the O37 ($O_{2sp}{}^3$) and O86 (O'_{4sp3}) heteroatoms were respectively

the main HB anchor points for AM5G—$4H_2O$ and AMP5G—$4H_2O$. These results have been consistent with those obtained by [6]. In addition, the energy parameters of the different complexes were analyzed. They are grouped in Table 11.

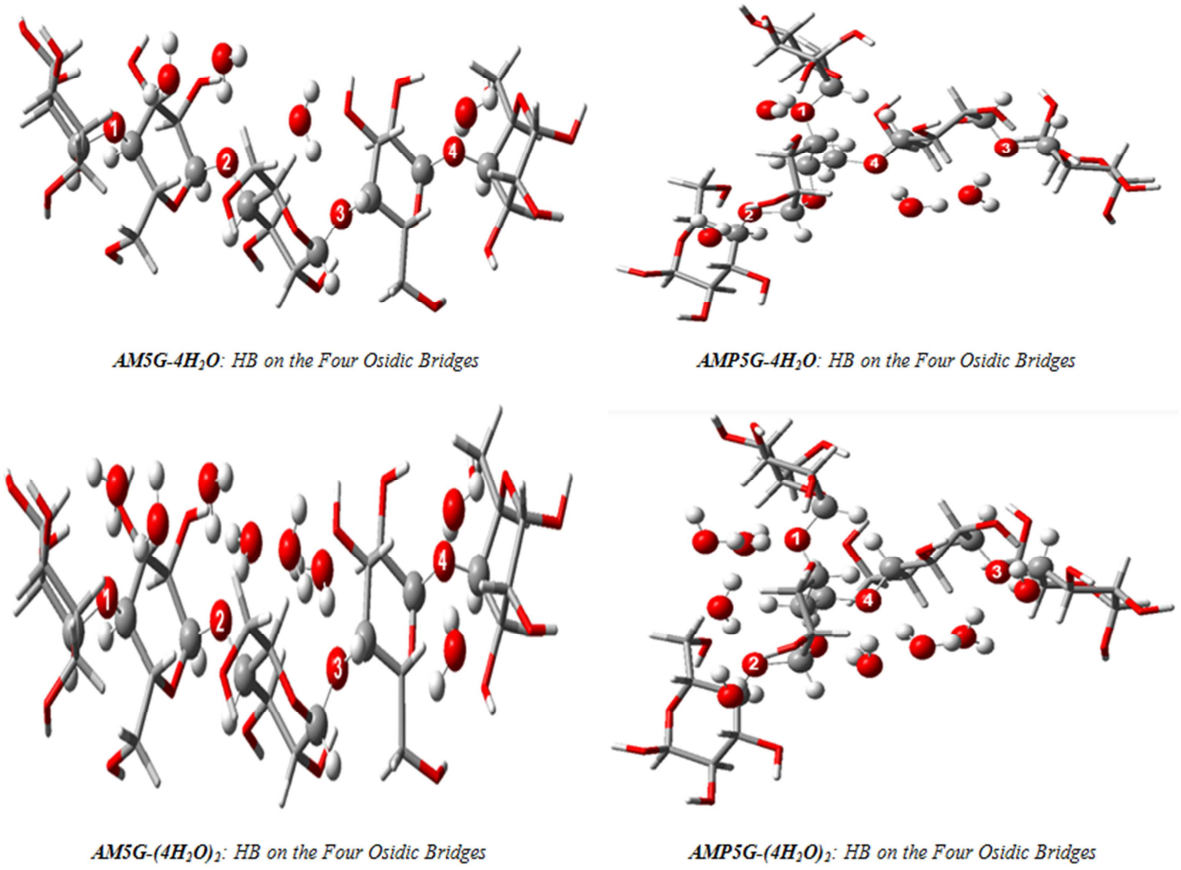

Figure 8. *Optimized Geometries of Complexes at ONIOM Level (B3LYP/6-311++G(d, p): AM1).*

Table 10. *Geometric Parameters of the AM5G—$4H_2O$ and AMP5G—$4H_2O$ Complexes at ONIOM Level (B3LYP/6-311++G(d, p): AM1).*

AM5G-$4H_2O$	α (°)	β (°)	d (Å)	AMP5G-$4H_2O$	α (°)	β (°)	d (Å)
O14 (O_1sp^3)	171.505	113.236	1.931	O14 (O'_1sp^3)	165.149	111.889	1.886
O37 (O_2sp^3)	176.254	127.802	1.825	O35 (O'_2sp^3)	168.469	128.193	1.951
O58 (O_3sp^3)	173.499	120.026	1.964	O78 (O'_3sp^3)	168.234	112.062	1.954
O79 (O_4sp^3)	164.573	111.817	1.851	O86 (O'_4sp^3)	158.155	117.086	1.874

4.2.2. Energy Parameters

The energy parameters were related to the AM5G—$4H_2O$ and AMP5G—$4H_2O$ complexes. The enthalpy values $\Delta_rH°_{298}$ were negative; the HB formation processes were exothermic. That of AM5G-$4H_2O$ and AMP5G-$4H_2O$ was non-spontaneous at 298 K according to the thermodynamic quantities Δ_rS and Δ_rG. The AM5G-$4H_2O$ complex was more stable than AMP5G-$4H_2O$. The free enthalpies of reaction were deviated by 5.618 kcal/mol. Its change was small (1.409 kcal/mol).

The degradation process of AM5G was facilitated compared to AMP5G. This result has been in accord with those of [2]; for the same molecular weight; the alteration of amylose has been faster than that of amylopectin. The study was focused on the spectroscopic parameters of the complexes.

Table 11. *Energy Parameters (kcal/mol) and Entropy (cal/mol. K-1) of the AM5G—$4H_2O$ and AMP5G—$4H_2O$ Complexes at ONIOM level (B3LYP/6-311++G(d,p): AM1).*

Complexes	$\Delta_rH°_{298}$	$\Delta_rS°_{298}$	$\Delta_rG°_{298}$
AM5G-$4H_2O$	-36.734	-145.067	6.519
AMP5G-$4H_2O$	-31.116	-130.951	7.928

4.2.3. Spectroscopic Parameters

The vibration frequencies Δϑ (O-H) of the different osidic bridges attributed to the AM5G—$4H_2O$ and AMP5G—$4H_2O$ complexes are grouped in Table 12. All the Δϑ (O-H) were positive. For the AM5G, the highest Δϑ (O-H) was associated with that of the O37 (O_2sp^3). Its related wave number was 299.91 cm^{-1}. This oxygen was the preferred site for establishing an HB within AM5G. The team's previous results were confirmed [2]. The O14 (O'_{1sp3}) atom was that of AMP5G. Furthermore, the probable HB of the complexes were explored with the NBO analysis.

Table 12. *Vibration Frequencies $\Delta\vartheta_{O-H}$ (cm^{-1}) of the AM5G—4H₂O and AMP5G—4H₂O Complexes at ONIOM Level (B3LYP/6-311++G(d, p): AM1).*

AM5G	Δϑ (O–H) cm^{-1}	AMP5G	Δϑ (O–H) (cm^{-1})
O14 (O_1sp^3)	291.22	O14 (O'_1sp^3)	320.36
O37 (O_2sp^3)	299.91	O35 (O'_2sp^3)	149.55
O58 (O_3sp^3)	259.12	O78 (O'_3sp^3)	162.94
O79 (O_4sp^3)	290.55	O86 (O'_4sp^3)	298.01

4.2.4. NBO Calculations on AM5G—4H₂O and AMP5G—4H₂O Complexes

Intermolecular and intramolecular interactions were concerned. The atomic numbers of these complexes are shown in Figure 9. They are displayed in Tables 13 and 15.

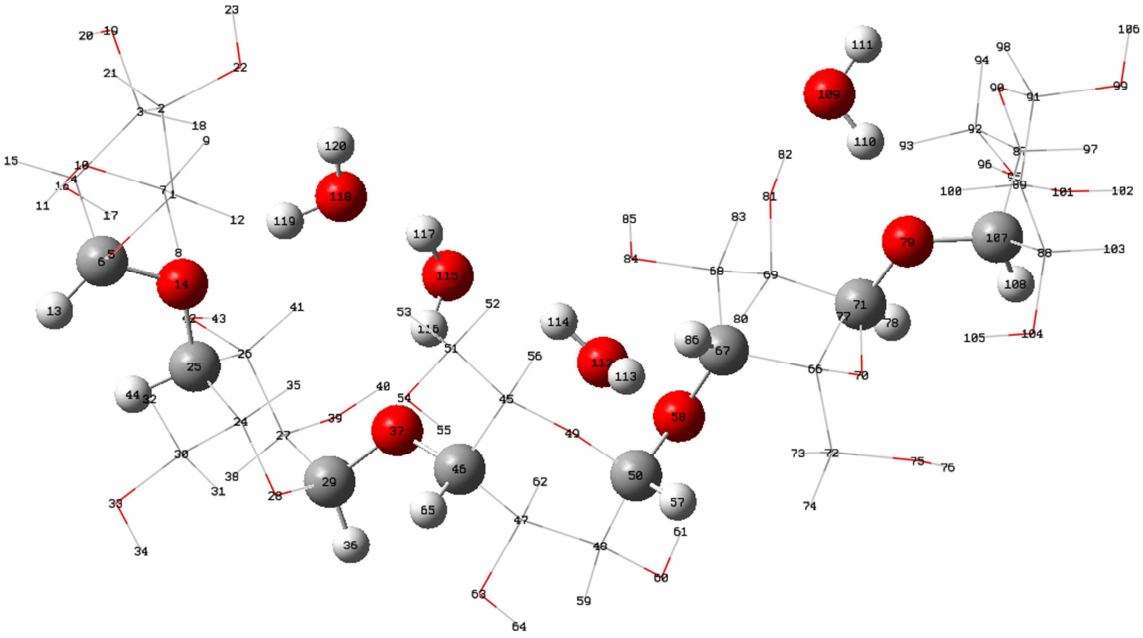

AM5G-4H₂O

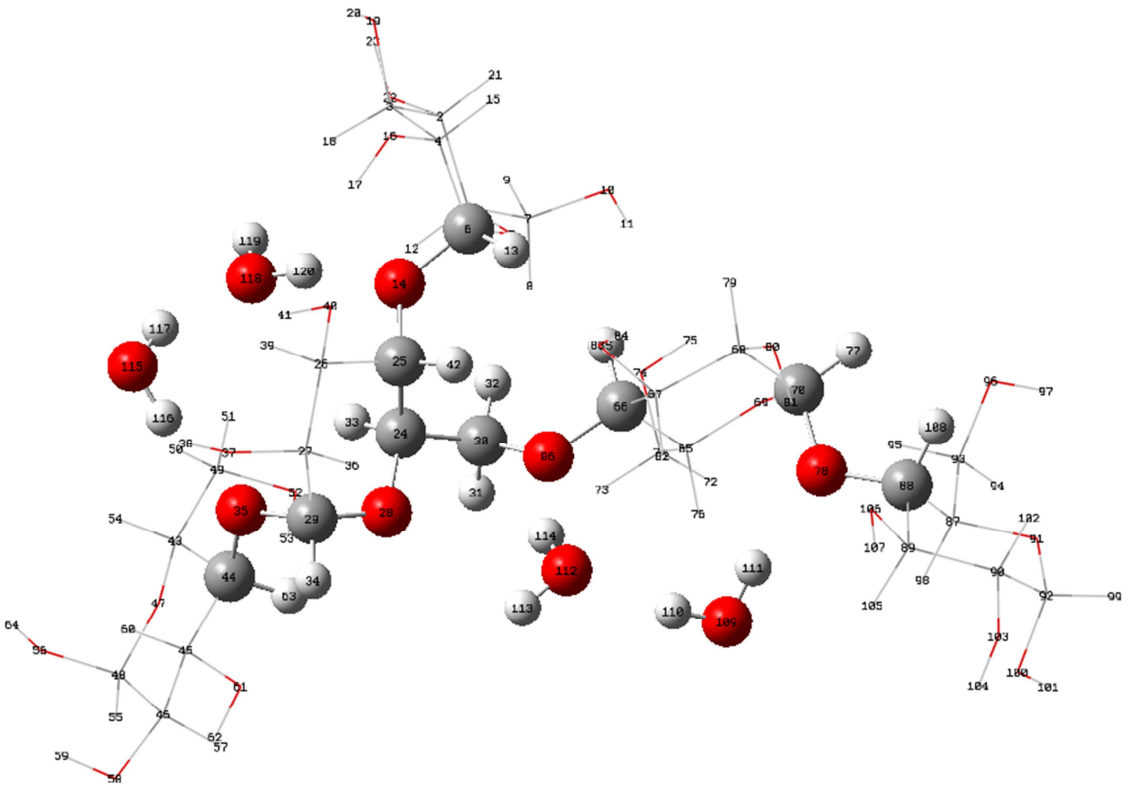

AMP5G-4H₂O

Figure 9. *Gauss Views 06 Software Numbering Adopted for NBO Analysis of AM5G-4H₂O and AMP5G-4H₂O Complexes.*

(i). NBO Analysis of the AM5G—4H_2O and AMP5G—4H_2O Complexes Intermolecular Interactions

The most important intermolecular CT for the AM5G-4H_2O complex was the osidic bridge O37. It was associated with the interaction $LP_1\ (O_{37}) \rightarrow \sigma^*(O_{115} - H_{116})$. Its stabilization energy was E^2= 8.97 kcal/mol. Its C.T was 14.50 a.u. The HB on this oxygen was the strongest. The value of D.E. around it was 1.94622e; its lone pairs were the most available in this direction. The preferred site for HB within AM4G was represented by it. The work of [2] is corroborated with this result.

For AMP5G-4H_2O, the most important intermolecular C.T was fixed to the O14 saccharide bridge. It was associated with the interaction $LP_1\ (O_{14}) \rightarrow \sigma^*(O_{118} - H_{120})$. Its stabilization energy was E^2 = 7.56 kcal/mol. The associated HB was the most solid. This atom had lone pairs because its E.D value was high. It was equal to 1.94673 rds. The main anchor point of HB within AMP5G was linked to O14.

The rupture of AM5G and AMP5G was respectively begun on the O37 and O14 heteroatoms. The AM5G was initially divided into tri- and disaccharides, according to NBO analysis data on intermolecular interactions. Then, each of the second compounds was further degraded into monosaccharides. AMP5G was broken up into monosaccharides and tetrasaccharides; these latter were in this order transformed into trisaccharides and monosaccharides. Finally, the trisaccharides were separated into di- and monosaccharides. The main results of the previous study are summarized in Table 14.

Table 13. *Second-Order Perturbation Energies E^2 (kcal/mol), C.T and E.D for the Transitions Intermolecular in the AM5G—4H_2O and AMP5G—4H_2O Complexes.*

Intermolecular interactions between AM5G—H_2O and AMP5G—H_2O										
Complexes	**NBO DONOR (i)**			**NBO ACCEPTOR (j)**						
	Donor	**Type**	**E. D (electron)**	**Acceptor**	**Type**	**E.D (electron)**	**E^2 (kcal/mol)**	**E (j)—E (i) (a. u)* ***	**F (i, j) (a. u)**	**C.T* 10^3**
AM5G-4H_2O	FP*(1) O14	π	1.95059	O118-H119	σ*	1.99417	5.79	0.99	0.068	9,44
	FP(2) O14	σ	1.91503	O118-H119	σ*	1.99417	0.79	0.76	0.022	1.68
	FP(1) O37	π	1.94622	O115-H116	σ*	1.99393	8.97	1.01	0.086	14.50
	FP(2) O37	σ	1.91748	O115-H116	σ*	1.99393	1.49	0.77	0.031	3.24
	FP(1) O58	π	1,95778	O112-H113	σ*	1.9952	4.22	1.05	0.060	6,53
	FP(2) O58	σ	1.91204	O112-H113	σ*	1.9952	2.12	0.79	0.037	4.39
	FP(1) O79	π	1.95029	O109-H110	σ*	1.99457	7.61	1.02	0.079	12.00
	FP(2) O79	σ	1.91406	O109-H110	σ*	1.99457	1.63	0.76	0.032	3.55
AMP5G-4H_2O	FP(1) O14	π	1.94891	O118-H120	σ*	1.99366	7.56	1.00	0.078	12.17
	FP(2) O14	σ	1.91538	O118-H120	σ*	1.99366	0.25	0.76	0.013	0.59
	FP (1) O35	π	1.95514	O115-H116	σ*	1.99561	5.45	1.05	0.068	8.39
	FP (1) O78	π	1.95424	O109-H111	σ*	1.99486	4.95	1.05	0.065	7.66
	FP (1) O86	π	1.95171	O112-H114	σ*	1.99570	6.52	1.02	0.073	10.24
*FP: free pair**a.u: atomic unit										

Table 14. *Key Research Findings Associated with AM5G and AMP5G.*

Associated criteria	**Most likely site of the HB for AM5G**	**Most likely site of the HB for AMP5G**
Geometry: distance	O37 (O_2sp^3)	O86 (O'_4sp^3)
Free Enthalpy	AM5G was degraded more easily than AMP5G	
Spectroscopy	O37 (O_2sp^3)	O14 (O'_1sp^3)
NBO analysis: intermolecular	O37 (O_2sp^3)	O14 (O'_1sp^3)
Results	O37 (O_2sp^3)	O14 (O'_1sp^3) and O86 (O'_4sp^3)

(ii). NBO Analysis of the AM5G—4H_2O and AMP5G—4H_2O Complexes Intramolecular Interactions

The E.D around the osidic bridges bonds are displayed in Table 15. Their intermolecular interactions were identified after the formation of HB. For the AM5G, four breakouts happened, according to the D.E. minimal rule. The former was occurred next to the O14; the O14-C25 binding was concerned. Its E.D was equalled to 1.98425e. It was lower than that of the C6-O14 link. The second was taken place near the O37 atom on the O37-C46. The third were spotted around the O58 oxygen. The connection O58-C67 was involved. The latest appeared on the O79 bubble; The O79-C107 binding was implicated.

Table 15. *The Intramolecular Bonds' E.D. Associated with Osidic Bridges of the AM5G and AMP5G.*

Molecules	**Sites**	**Link**	**Type**	**E.D. (electron)**
AM5G	O14	C6-O14	σ	1.98846
		O14-C25	σ	1.98425
	O37	C29-O37	σ	1.98817
		O37-C46	σ	1.98560
	O58	C50-O58	σ	1.98767
		O58-C67	σ	1.98606
	O79	C71-O79	σ	1.98826
		O79-C107	σ	1.98631
AMP5G	O14	C6-O14	σ	1.98855
		O14-C25	σ	1.98540
	O35	C29-O35	σ	1.98779
		O35-C44	σ	1.98474
	O78	C70-O78	σ	1.98800

Molecules	Sites	Link	Type	E.D. (electron)
		O78-C88	σ	1.98467
	O86	C30-O86	σ	1.98962
		O86-C66	σ	1.98557

According to the ED values, the alteration happened at O14-C25 of the AMP5G. This mentioned bonding was broken up at the O14; the final split was occurred in the O35-C44 connection near O35. Similarly, for the O78 osidic bridge, the scission was located at the O78-C88 one. Ultimately, the O86-C66 linkage was interrupted next to the O86. The major preferred sites of HB within the five-building blocks of amylose, and of amylopectin were identified by using the NBO analysis. Moreover, the bonds responsible for the cleavage of polysaccharides were revealed by the last method. Furthermore, the additional H_2O and synthons effects on the osidic bridges geometry were investigated.

4.2.5. Geometry of AM5G — $(4H_2O)_2$ et AMP5G — $(4H_2O)_2$ Complexes

The effects were linked to the interactions of one then two H_2O on each saccharide bridge of the following complexes: AM5G-H_2O, AM5G-2H_2O, AMP5G-H_2O and AMP5G-2H_2O.

(i). Complexes Associated with Amylose

The cleavage bonds of AM5G were highlighted. Their lengths and valence angles are shown in Table 16.

Table 16. *Bond Lengths d(Å) and Valence angle θ (°) Related to the Osidic Bridges of the AM5G, AM5G—H_2O and AM5G—2H_2O Complexes.*

Distances	Angles	AM5G	AM5G-H_2O	AM5G-2H_2O	Δd_1	$\Delta\theta_1$	Δd_2	$\Delta\theta_2$
d (C6-O14)		1.43	1.43	1.45	0.00		0.02	
d (O14-C25)		1.43	1.45	1.45	0.02		0.02	
	θ(C-O-C)	117.80	119.95	116.33		2.16		-1.46
d (C29-O37)		1.43	1.42	1.44	0.00		0.01	
d (O37-C46)		1.43	1.44	1.45	0.01		0.02	
	θ(C-O-C)	116.43	117.61	117.54		1.18		1.10
d (C50-O58)		1.42	1.43	1.43	0.01		0.01	
d (O58-C67)		1.44	1.44	1.44	0.00		0.00	
	θ(C-O-C)	116.39	116.17	117.66		-0.22		1.26
d (C71-O79)		1.43	1.43	1.45	0.00		0.02	
d (O79-C107)		1.43	1.45	1.47	0.02		0.04	
	θ(C-O-C)	117.80	118.22	113.85		0.42		-3.94

The distances have been increasing as an H_2O neared to each osidic bridge. For the O14 oxygen, the highest value occurred on O14-C25 with Δd1 = 0.02 Å. This variation was accentuated when two H_2O approached this site. It became Δd2 = 0.02 Å. The breakup at this O14 started with O14-C25 cross-linkage. For the O37, the O37-C46 binding was the relevant bond in the AM4G—H_2O complex. It was stretched from Δd1 = 0.01 Å to Δd2 = 0.02 Å when two H_2O were moved simultaneously on this bridge. The mentioned connection resulted from the AM5G to split into O37. For the O58 atom, the greatest value of Δd1 was around the C50-O58 (0.01 Å) link. The d2 distance extended by Δd2 = 0.01 Å because of the proximity of the two H_2O to O58. The rupture at this last took place at the C50-O58 bond. Finally, for the O79 oxygen, it concerned the O79-C107 connection; its length increased when two H2O molecules approached this latter atom. The breakup happened at the O79-C107 binding.

For AM5G, the cleavage at the O14 osidic bridge began at the O_{14}-C_{25} bond. That of the O37 was initiated at the O37-C46 one. Regarding the O58 oxygen, the opening occurred at C50-O58 cross-link. That of O79 atom was lunched at O79-C107 binding. The result on the C50-O58 was determined by the NBO analysis. Simply, the split around in the mentioned attachment was missing. On the other hand, those linked to the O14-C25, O37-C46 and O79-C107 bindings were confirmed. Its complexation with one to two H_2O had insufficiently influenced on the valence angles associated with the O14, O37, O58 and O79 osidic bridges. Δθ1 was corresponded to 2.16° at most. For the first H_2O, $|\Delta\theta_2$ | was equalled to 3.95°. The effects relating to the interactions of water molecules and the five-synthon amylopectin (AMP5G) are also examined.

(ii). Complexes Associated with Amylopectin Binding

The distances between the carbon and the oxygen of the osidic bridges are collected in Table 17. The associated valence angles are also displayed. The simultaneous interaction of an H_2O and this AMP5G bridge's atom had increased them. The O14-C25 bond was extended by Δd1 = 0.01 Å compared to O14 oxygen. This increase was reinforced when another H_20 was added. The Δd1 became Δd2 = 0.02 Å. That of O35 was risen to Δd1 = 0.01 Å in the AMP5G-H_2O complex. It had reached Δd2 = 0.01 Å for both H_2O. The O35-C44 binding was the cleavage site on this osidic bridge. For the O78 oxygen, the responsible was the O78-C88 bond. The elongation was doubled. It goes from Δd1 = 0.01 Å to Δd2 = 0.02 Å. For O86 atom, the biggest value of Δd1 was appeared near O86-C66 (Δd1 = 0.01 Å) in AMP5G-H_2O. The interaction of the two H_2O on the O86 oxygen was caused by the elements of this link. The latter stabilized at Δd2 = 0.02 Å. It was broken at the bridge O86. The ruptures around O14-C25, O35-C44 and O78-C88 connections were also highlighted by the NBO analysis.

For AMP5G, the geometric parameters were partially identical to those obtained with the NBO analysis; the HB were formed around the O14-C25, O35-C44, and O78-C88 bonds. However, this last method was ignored that of C30-O86 cross-linkages. These results and the effects of the H_2O on the

AM5G and AMP5G osidic bridges are summarized in Table 18. At the end of the study on the five amylose and amylopectin synthons, the order of their cleavage was elucidated. It is illustrated in Figure 10 in the schema form.

Table 17. *Bond Lengths d(Å) and Valence angles θ (°) Related to the Osidic Bridges of the AMP5G, AMP5G—H_2O and AMP5G—$2H_2O$ Complexes.*

Distances	Angles	AMP5G	AMP5G-H_2O	AMP5G-$2H_2O$	Δd_1	$\Delta\theta_1$	Δd_2	$\Delta\theta_2$
d(C6-O14)		1.42	1.43	1.42	0.01		0.00	
d(O14-C25)		1.44	1.45	1.45	0.01		0.02	
	θ(C-O-C)	118.60	119.26	119.22		0.66		0.62
d(C29-O35)		1.43	1.43	1.44	0.00		0.01	
d(O35-C44)		1.44	1.46	1.45	0.02		0.01	
	θ(C-O-C)	114.92	115.38	114.42		0.46		-0.50
d(C70-O78)		1.43	1.43	1.44	0.00		0.01	
d(O78-C88)		1.43	1.44	1.45	0.01		0.02	
	θ(C-O-C)	117.55	118.02	117.43		0.47		-0.12
d(C30-O86)		1.42	1.43	1.44	0.01		0.02	
d(O86-C66)		1.43	1.44	1.44	0.01		0.01	
	θ(C-O-C)	117.44	118.18	116.84		0.74		-0.59

Table 18. *Key Research Findings Associated with the AM5G—$4H_2O$ and AMP5G—$4H_2O$ Complexes.*

Associated criteria	Liaisons responsible for the AM5G split	Liaisons responsible for the AMP5G split
NBO analysis: intramolecular	O14-C25, O37-C46, O58-C67 and O79-C107	O14-C25, O35-C44, O78-C88 and O86-C66
Effects of H_2O	O14-C25, O37-C46, C50-O58 and C71-O79	O14-C25, O35-C44, O78-C88 and C30-O86
Conclusion	O14-C25, O37-C46, C50-O58 and O79-C107	O14-C25, O35-C44, O78-C88 and C30-O86

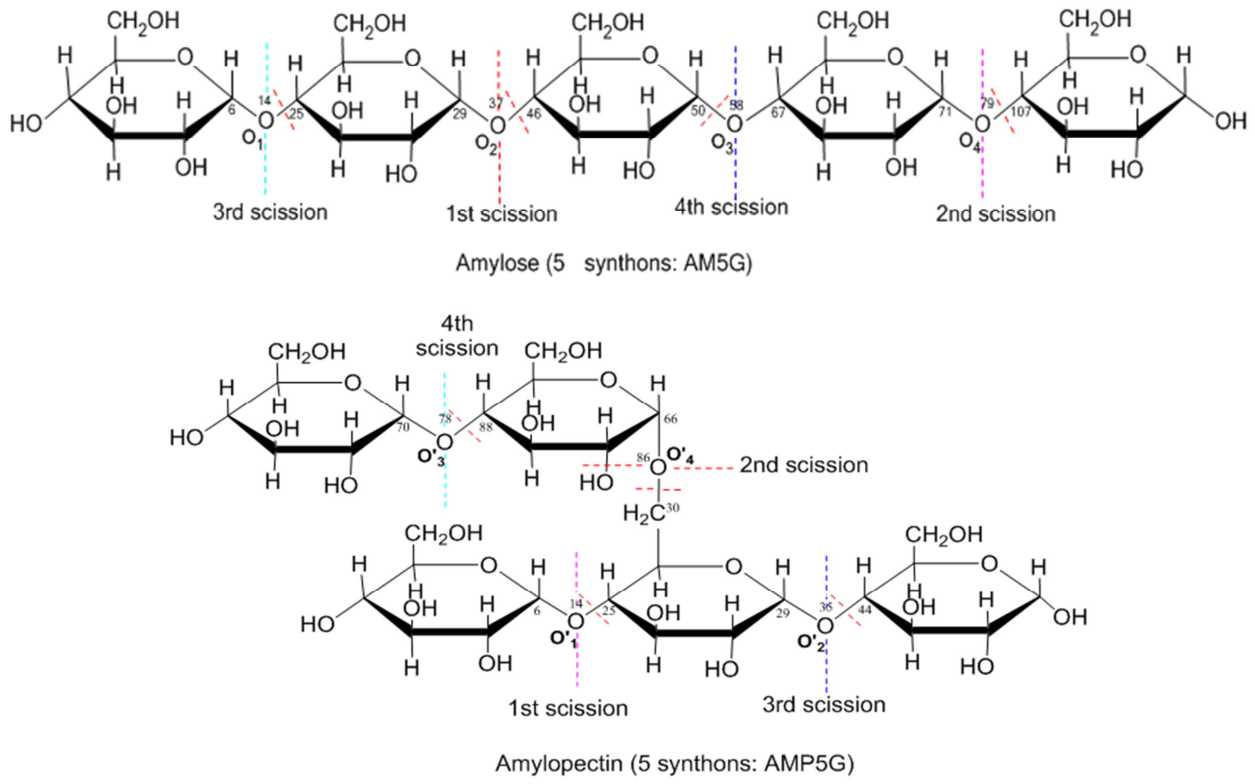

Figure 10. *Scission Order of Amylose and Amylopectin with Five Synthons.*

5. Conclusion

The description of the bonds responsible for the polysaccharides alteration in plantain starch is the objective of this article. The attack of two water molecules was discussed. The four- and five-block D-glucose amylose and amylopectin chains were reduced. The two-layer ONIOM method at the ONIOM level (B3LYP/6-311++G(d,p): AM1) for the complex formation was employed. NBO analyzes were also used. The geometrical, energetic, and spectroscopic parameters related to the different polysaccharide-water structures were supplied by the calculations. Similarly, intermolecular stabilization and intramolecular E.D energies were provided by the NBO technique. The preferred HB sites of amylose, or amylopectin were highlighted by processing these data. In addition, the bonds responsible for cleavage in each polysaccharide were established.

The O37 (O_2sp^3) and O63 (O'_{3sp3}) oxygen are respectively the HB creation points for AM4G and AMP4G. The first atom is the AM5G favourite HB receptor. The O14 (O'_{1sp3}) and O86(O'_{4sp3}) ones are those of AMP5G. Moreover, amylose is always degraded before amylopectin. The sites capable of forming HB are increased by the elongation of the synthon chain. The bonds responsible for the cleavage in each polysaccharide are revealed by the simultaneous interaction of two H_2O molecules on every osidic bridge. Thus, the rupture of AM4G took place around the O14-C25, O37-C46 and O58-C67 bindings. The O13-C21, O55-C65 and O63-C43 cross-link are those of AMP4G. For AM5G, the sites of its fragmentation are on the O14-C25, O37-C46 and C50-O58 and O79-C107 ones. For AMP5G, they are located at O14-C25, O35-C44, O78-C88 and C30-O86 bonds. In a word, the results obtained and discussed here make it possible to identify the sites of polysaccharide degradation under the action of water. They suggest providing chemical structures that prevent the osidic bridges from associating with electrophiles as hydrogen. The study of this process will constitute the main perspective of this work.

References

[1] Yao K. Augustin, Koffi Djary M., Zaouli B. Irié and Niamké L. Sébastien. 2004. Effet de la substitution partielle de la farine de blé par la purée de la banane plantain (Musa AAB) bien mûre sur la qualité des produits de pâtisserie. J. Applied Biosci, 82, 7436–7448. https://doi.org/10.4314/jab.v82i1.12

[2] Cordenunsi B. R. and Lajolo FM. 1995. Starch breakdown during banana ripening: sucrose synthase and sucrose phosphate synthase. J. Agric. Food Chem., 43, 363–372. https://doi.org/10.1021/jf00050a016

[3] Lepengue Alexis N., Mouaragadja Isaac, Dick Emmanuel, Mbatchi Bertrand and Aké Sévérin. 2010. Amélioration de la durée de conservation des bananes plantain aux températures ambiantes, Int. J. Biol. Chem. Sci. 4(3), 730–737.

[4] Able Anoh Valentin, N'Guessan Boka Robert and Bamba El-Hadji Sawaliho. 2020. Monosaccharide Degradation Analysis by Functional Density Theory at Level B3lyp/6-311G (d, p). Op. Acc. J. Bio. Sci and Res, 6(2). DOI: 10.46718/JBGSR.2020.06.000144.

[5] Momany F. A, Appell M., Starti G., and Willett J. L. 2004. B3LYP/6-311++G** study of monohydrates of α- and β-D-glucopyranose: hydrogen bonding, stress energies, and effect of hydration on internal coordinates. Carbohydr. Res., 338, 553–567. https://doi.org/10.1016/j.carres.2003.10.013.

[6] Able Anoh Valentin, N'Guessan Boka Robert and Bamba El-Hadji Sawaliho. 2021. Hydrogen Bonds Sites of Amylose or Amylopectin from Starch at the ONIOM Level (B3LYP/6-311++G [d, p]: AM1). Computational Chemistry, 9, 85–96. DOI: 10.4236/cc.2021.91005.

[7] Lachi Nadia. 2015. Étude des Complexes d'inclusion par la méthode ONION. Guelma (Algérie): Université, 8 mai 1945, Faculté des mathématiques et de l'informatique et des sciences de la matière.

[8] Theivarasu C. and Murugesan R., 2016. «Natural bond orbital (NBO) population analysis of an energetic molecule 1-phenyl-2-nitroguanidine,» Int. J. Chem. Sci., 14 (14), 2019-2050.

[9] Michael J. Frisch, G. W. Trucks, H. B. Schlegel, G. E. Scuseria, M. A. Robb and D. J. Fox. 2009, Gaussian09, Revision D. 01. Gaussian Inc., Wallingford, CT.

[10] Jeffrey G. A. and Seanger W. 1991. Hydrogen Bonding in Biological Structures, Springer Berlin. https://doi.org/10.1007/978-3-642-85135-3

[11] Rowland R. S. and Taylor R. 1996. Intermolecular nonbonded contact distances in organic crystal structures: Comparison with distances expected from Van der Waals radii, J. Phys. Chem. 100, 7384–7391. https://doi.org/10.1021/jp953141+

[12] Jorly J. and Eluvathingal D. J. 2007. Red-, Blue-, or No-Shift in Hydrogen Bonds: A Unified Explanation. Journal of the American Chemical Society, 129, 4620–4632. https://doi.org/10.1021/ja067545z

[13] Bondi A. 1964. Van der Waals volumes and radii J. Phys. Chem., 68, 441–451. https://doi.org/10.1021/j100785a001

[14] Desiraju G. R. and Steiner T., 1999. The Weak Hydrogen Bond: In Struct. Chem. and Biol. (Oxford University Press.)